Performance evaluation of an active headrest using the remote microphone technique

Debi Prasad Das (1,2), Danielle J. Moreau (1) and Ben Cazzolato (1)

(1) School of Mechanical Engineering, The University of Adelaide, SA 5005, AUSTRALIA
(2) PE&I Cell, CSIR-IMMT, Bhubaneswar, Orissa 751013, INDIA

ABSTRACT

Active headrests produce a quiet zone near the occupant's head using active noise control. It has been shown that active headrest algorithms using virtual microphones are better than those using physical microphones, as they have the ability to shift the zone of quiet away from the location of the physical microphones towards the ears of the occupant. Recently, the virtual microphone arrangement based ANC method was used for an active headrest application, in which it was assumed that the primary pressures at the physical and virtual microphone locations are similar. In this paper the previous work is extended to incorporate the remote microphone technique, which is a better estimation algorithm as it uses an extra transfer function between the physical and virtual microphone. Experiments using two secondary speakers, and two physical and two virtual microphones are carried out to compare the results from both algorithms. Details of the multichannel virtual microphone algorithm for an active headrest are given in this paper along with the experimental results.

INTRODUCTION

An active headrest is a system which gives comfort from unwanted noise by producing a quiet zone near an occupant's head using active noise control (ANC) (Nelson and Elliot, 1992, Kuo and Morgan, 1996, Hansen & Synder, 1997). ANC works on the principle of generating antinoise though a speaker system to cancel the primary noise by acoustic superposition. In the case of an active headrest, the speaker system generally consists of two loudspeakers placed close to the head to generate the antinoise. An active headrest also employs two microphones on either side of the head to sense the primary noise level. The ANC controller has the objective of minimizing the noise at these two microphones.

In short, the active headrest system is a two speaker, two microphone ANC system which uses either a reference microphone signal (feed-forward control) or an internally estimated signal (feedback or internal model control). The control algorithm minimizes the two physical microphone signals to generate a quiet zone located at the physical microphone positions. In an attempt to move the zone of quiet from the physical microphone locations to the locations of the occupant's ears, various algorithms have been proposed. These algorithms are named virtual sensing algorithms. These algorithms estimate the noise signal at the ear or virtual microphone location using the noise signal at the physical microphones placed away from the ears. The effectiveness of ANC at the virtual locations greatly depends on the accuracy of the virtual microphone signal estimate. A number of virtual sensing algorithms have been proposed for active noise control in the past including the virtual microphone arrangement (VMA) (Elliott and David, 1992), the remote microphone technique (RMT) (Roure and Albarrazin, 2000), the forward-difference prediction technique (Cazzolato, 1999), the adaptive LMS virtual microphone technique (Cazzolato, 2002), the Kalman filtering virtual sensing technique (Petersen et al., 2008) and the stochastically optimal tonal diffuse field (SOTDF) virtual sensing method (Moreau et al. 2009).

Garcia-Bonito et al. (1997) proposed a local active headrest system which uses the virtual microphone arrangement (VMA). This virtual sensing algorithm uses the assumption that the primary pressure at the physical and virtual microphone locations is similar. Brodband performance of the active headrest has been studied by Rafaely et al. (1999). A robust controller using H_2/H_∞ feedback control has been proposed for a robust active headrest system (Rafaely and Elliott, 1999). This approach is focused on noise control at the physical microphones. Holmberg et al. (2002) used pole-placement design to actively control noise at a virtual location in a headrest. Various performance limits and the real-time implementation of a virtual microphone active headrest have been presented by Tseng et al. (2002). Pawelczyk (2002a, 2002b, 2003a, 2003b, 2004) presented various types of active headrest algorithms. Pawelczyk (2004) and Brothanek and Jiricek (2002) have proposed virtual headrest systems that use an extra reshaping filter to estimate the virtual microphone signal from the physical microphone signal.

The VMA (Elliott and David, 1992) has become increasingly popular and is used in many headrest systems (Pawelczyk, 2002a, 2002b, 2003a, 2003b, 2004). However, in the VMA, it is assumed that the primary pressure at the physical and virtual microphone locations is similar. This is the case when the microphones are located in the far-field of a noise source. However, active headrest systems based on VMA are not effective when placed near to the noise source as the physical and virtual microphones do not receive the same acoustic pressure signal. The RMT technique (Roure and Albarrazin, 2000) uses an extra transfer function to estimate the primary noise signal at the virtual location from the primary noise signal at the physical location and is shown to be more accurate in estimating the overall sound pressure at virtual location. In this paper we propose a new headrest system based on internal model control using the RMT technique to control near field sound and generate a quiet zone at the occupant's ear.

A multichannel algorithm with two control speakers and two physical microphones is proposed in this paper. The algorithm is implemented in real time to actively control a near-field noise source around an artificial head. Two microphones are located inside the ears of the artificial head (which is the desired or virtual location). Three dimensional scanning is done to evaluate the zone of quiet around the head. In this paper, the performance of three algorithms is compared; ANC controlling the physical microphone signal (termed as local ANC), virtual ANC with the VMA technique (Pawelczyk, 2003) and the proposed virtual ANC algorithm with the RMT.

The organization of the paper is as follows. In Section II, the complete algorithm is presented. Section III shows block diagrams of two previously employed ANC algorithms which are compared experimentally in this paper. Experimental setup and the results are presented in Section IV and V respectively. The Conclusion is presented in Section VI.

PROPOSED ACTIVE HEADREST ALGORITHM

Estimating virtual error signal using RMT algorithm

The remote microphone technique (RMT) (Roure and Albarrazin, 2000), estimates the total error signal at the virtual location, $\hat{e}_v(n)$, using the error signal from a physical microphone, $e_p(n)$. The RMT requires a preliminary identification stage in which a second physical microphone is temporarily placed at the virtual location. Estimates of the secondary transfer functions at the physical and virtual locations, $\hat{S}_P(z)$ and $\hat{S}_v(z)$ respectively, are measured during the preliminary identification stage along with an estimate of the primary transfer function between the physical and virtual locations, $\hat{H}(z)$. In this paper, ^ symbol indicates the estimated quantities.

A block diagram of the remote microphone technique is given in Fig. 1. As shown in Fig. 1, an estimate of the primary disturbance, $\hat{d}_p(n)$, at the physical microphone is first calculated using

$$\hat{d}_p(n) = e_p(n) - \hat{y}_p(n) = e_p(n) - \hat{S}_p(z)y(n), \qquad (1)$$

where $\hat{y}_p(n)$ is an estimate of the secondary disturbance at the physical microphone and $y(n)$ is the control signal. Next, an estimate of the primary disturbance, $\hat{d}_v(n)$, at the virtual location is estimated as

$$\hat{d}_v(n) = \hat{H}(z)\hat{d}_p(n). \qquad (2)$$

Finally, an estimate, $\hat{e}_v(n)$, of the total virtual error signal from both sources is calculated using

$$\hat{e}_v(n) = \hat{d}_v(n) + \hat{y}_v(n) = H(z)\hat{d}_p(n) + \hat{S}_v(z)y(n), \qquad (3)$$

where $\hat{y}_v(n)$ is an estimate of the secondary disturbance at the virtual microphone. Thus an estimate of the virtual error signal has been calculated from the physical error signal.

RMT based ANC algorithm for Headrest

In the active headrest system, there are two loudspeakers (left and right) and correspondingly two physical microphones used as the error microphones. In an internal model control algorithm, the reference signal is estimated from the error microphones. This is also referred to as active feedback control. The control algorithm proposed here is an internal model control algorithm.

Notation Convention

$S^p{}_{LL}$: Secondary path from left control source to left physical microphone,

$S^p{}_{RL}$: Secondary path from left control source to right physical microphone,

$S^p{}_{LR}$: Secondary path from right control source to left physical microphone,

$S^p{}_{RR}$: Secondary path from right control source to right physical microphone,

$S^v{}_{LL}$: Secondary path from left control source to left virtual microphone,

$S^v{}_{RL}$: Secondary path from left control source to right virtual microphone,

$S^v{}_{LR}$: Secondary path from right control source to left virtual microphone,

$S^v{}_{RR}$: Secondary path from right control source to right virtual microphone,

$\hat{S}^p{}_{LL}$: Estimated secondary path from left control source to left physical microphone,

$\hat{S}^p{}_{RL}$: Estimated secondary path from left control source to right physical microphone,

$\hat{S}^p{}_{LR}$: Estimated secondary path from right control source to left physical microphone,

$\hat{S}^p{}_{RR}$: Estimated secondary path from right control source to right physical microphone,

$\hat{S}^v{}_{LL}$: Estimated secondary path from left control source to left virtual microphone,

$\hat{S}^v{}_{RL}$: Estimated secondary path from left control source to right virtual microphone,

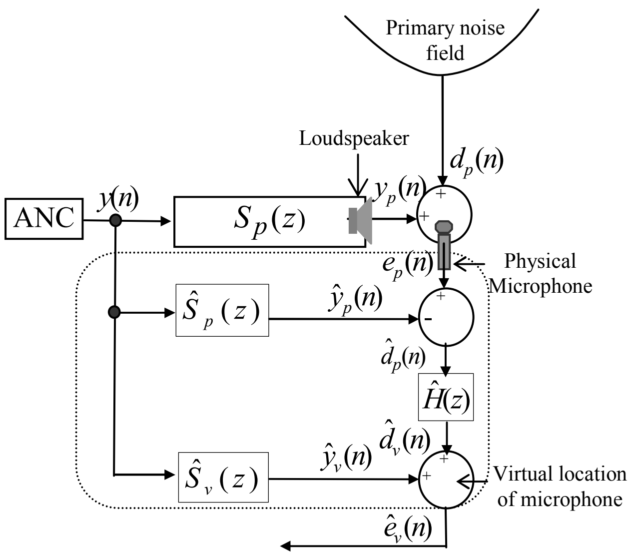

Figure 1 Remote microphone technique for estimating virtual error signal

$\hat{S}^{v}{}_{LR}$: Estimated secondary path from right control source to left virtual microphone,

$\hat{S}^{v}{}_{RR}$: Estimated secondary path from right control source to right virtual microphone,

$\hat{H}_{L}$: Estimated primary transfer function between left physical and left virtual microphone,

$\hat{H}_{R}$: Estimated primary transfer function between right physical and right virtual microphone,

$\hat{W}_{LL}$: Adaptive filter to generate part of the signal to the left control source and driven by the left reference signal,

$\hat{W}_{LR}$: Adaptive filter to generate part of the signal to the right control source and driven by the left reference signal,

$\hat{W}_{RL}$: Adaptive filter to generate part of the signal to the left control source and driven by the right reference signal,

$\hat{W}_{RR}$: Adaptive filter to generate part of the signal to the right control source and driven by the right reference signal.

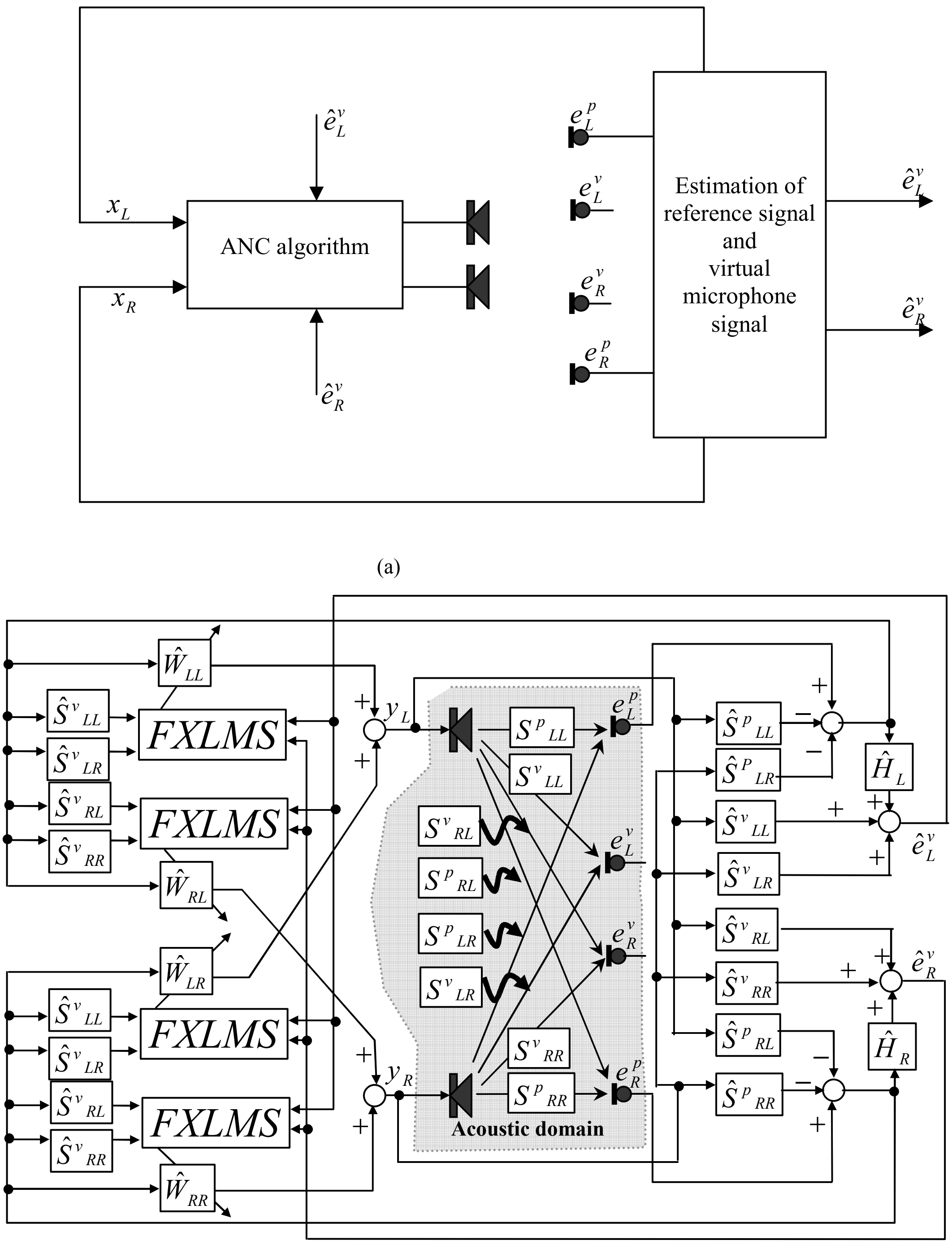

(a)

(b)

Figure 2 Active headrest algorithm (a) block diagram of virtual microphone control (b) detailed block diagram using remote microphone technique

The impulse response variables and their vectors are represented using lower case and lower case bold face font, respectively for all of the above transfer functions e.g. $s^{p}{}_{LL}$ and $\mathbf{s}^{p}{}_{LL}$ represent the impulse response variable and its vector corresponding to the transfer function $S^{p}{}_{LL}$.

y_L and y_R are left and right control signals respectively.

$\hat{x}_L$ and $\hat{x}_R$ are left and right estimated reference signals respectively.

e_L^p and e_R^p are physical error microphone signals of left and right sides respectively.

e_L^v and e_R^v are virtual error microphone signals of left and right sides respectively.

$\hat{e}_L^v$ and $\hat{e}_R^v$ are estimated virtual error microphone signals of left and right sides respectively.

These signals are also represented in their vector form (lower case bold font) which corresponds to a set of finite samples where the first element is the present sample, e.g. $\mathbf{y}_L(n) = [y(n), y(n-1),..., y(n-N+1)]$, where n is the sample index.

The four adaptive filters used as the controller, $\hat{W}_{LL}$, $\hat{W}_{LR}$, $\hat{W}_{RL}$ and $\hat{W}_{RR}$, are updated as follows using the estimated virtual error signals

$$\hat{\mathbf{w}}_{LL}(n+1) = \hat{\mathbf{w}}_{LL}(n) - \mu \mathbf{x}'_{LL\_L}\,\hat{e}_L^v(n) - \mu \mathbf{x}'_{RL\_L}\,\hat{e}_R^v(n)\,, \tag{1.a}$$

$$\hat{\mathbf{w}}_{RL}(n+1) = \hat{\mathbf{w}}_{RL}(n) - \mu \mathbf{x}'_{LR\_L}\,\hat{e}_L^v(n) - \mu \mathbf{x}'_{RR\_L}\,\hat{e}_R^v(n)\,, \tag{1.b}$$

$$\hat{\mathbf{w}}_{LR}(n+1) = \hat{\mathbf{w}}_{LR}(n) - \mu \mathbf{x}'_{LL\_R}\,\hat{e}_L^v(n) - \mu \mathbf{x}'_{RL\_R}\,\hat{e}_R^v(n)\,, \tag{1.c}$$

$$\hat{\mathbf{w}}_{RR}(n+1) = \hat{\mathbf{w}}_{RR}(n) - \mu \mathbf{x}'_{LR\_R}\,\hat{e}_L^v(n) - \mu \mathbf{x}'_{RR\_R}\,\hat{e}_R^v(n)\,. \tag{1.d}$$

where μ is the adaptation coefficient or step-size and

$$x'_{LL\_L}(n) = x_L(n) * \hat{s}^{v}{}_{LL}\,, \tag{2.a}$$

$$x'_{RL\_L}(n) = x_L(n) * \hat{s}^{v}{}_{RL}\,, \tag{2.b}$$

$$x'_{LR\_L}(n) = x_L(n) * \hat{s}^{v}{}_{LR}\,, \tag{2.c}$$

$$x'_{RR\_L}(n) = x_L(n) * \hat{s}^{v}{}_{RR}\,, \tag{2.d}$$

$$x'_{LL\_R}(n) = x_R(n) * \hat{s}^{v}{}_{LL}\,, \tag{3.a}$$

$$x'_{RL\_R}(n) = x_R(n) * \hat{s}^{v}{}_{RL}\,, \tag{3.b}$$

$$x'_{LR\_R}(n) = x_R(n) * \hat{s}^{v}{}_{LR}\,, \tag{3.c}$$

$$x'_{RR\_R}(n) = x_R(n) * \hat{s}^{v}{}_{RR}\,, \tag{3.d}$$

where * denotes the convolution operation.

The control signals to the left and the right speakers are generated as follows

$$y_L(n) = \mathbf{x}_L(n)\hat{\mathbf{w}}_{LL}(n)^T + \mathbf{x}_R(n)\hat{\mathbf{w}}_{LR}(n)^T\,, \tag{4.a}$$

$$y_R(n) = \mathbf{x}_L(n)\hat{\mathbf{w}}_{RL}(n)^T + \mathbf{x}_R(n)\hat{\mathbf{w}}_{RR}(n)^T\,. \tag{4.b}$$

The left and right primary reference signals are calculated according to

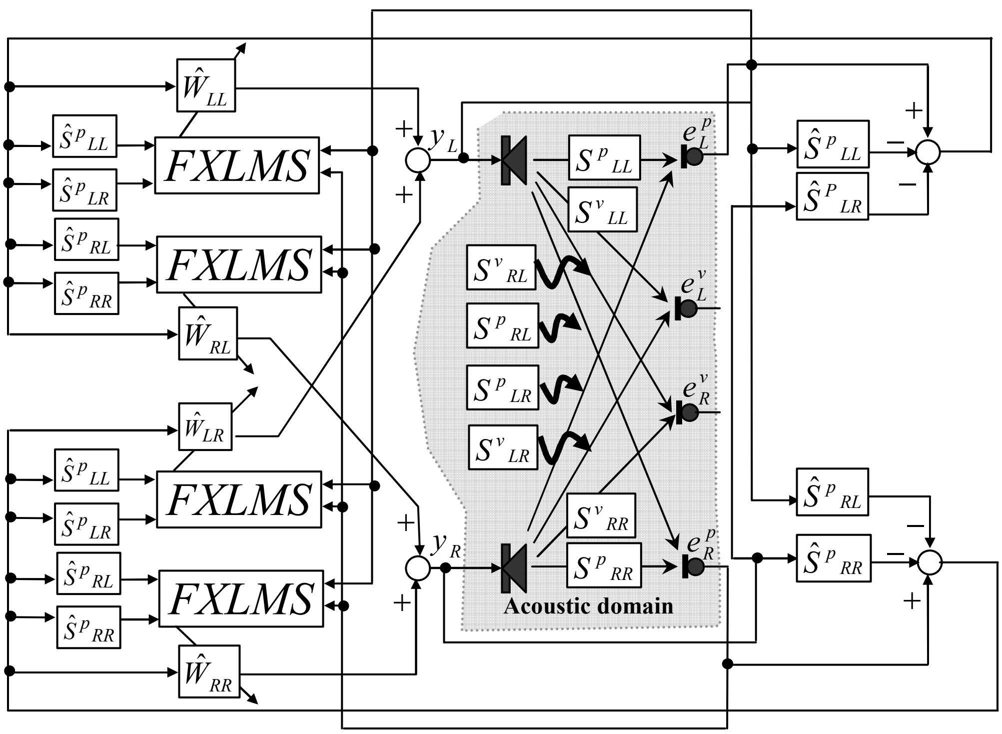

Figure 3 Active headrest algorithm controlling noise at physical microphones.

$$x_L(n) = e_L^p(n) - y_L(n) * \hat{s}^p{}_{LL} - y_R(n) * \hat{s}^p{}_{LR}\,, \quad (5.a)$$

$$x_R(n) = e_R^p(n) - y_L(n) * \hat{s}^p{}_{RL} - y_R(n) * \hat{s}^p{}_{RR}\,. \quad (5.b)$$

The virtual error signals are estimated as follows

$$\hat{e}^v{}_L(n) = y_L(n) * \hat{s}^v{}_{LL} + y_R(n) * \hat{s}^v{}_{LR} + x_L(n) * h_L\,, \quad (6.a)$$

$$\hat{e}^v{}_R(n) = y_L(n) * \hat{s}^v{}_{RL} + y_R(n) * \hat{s}^v{}_{RR} + x_R(n) * h_R\,. \quad (6.b)$$

The active headrest algorithm for virtual microphone control is shown in Fig. 2(a). This figure shows that a reference signal and virtual microphone signal estimation algorithm are required for ANC. The proposed RMT based active headrest algorithm is presented in Fig. 2 (b) in detail.

Estimation of Transfer functions

The performance of the active headrest system greatly depends on accurate estimation of the various transfer functions, $\hat{S}^p{}_{LL}$, $\hat{S}^p{}_{RL}$, $\hat{S}^p{}_{LR}$, $\hat{S}^p{}_{RR}$, $\hat{S}^v{}_{LL}$, $\hat{S}^v{}_{RL}$, $\hat{S}^v{}_{LR}$, $\hat{S}^v{}_{RR}$, $\hat{H}_L$ and $\hat{H}_R$. These transfer functions are estimated in three stages. In stage-1, the left loudspeaker is excited with white noise. With the signals received by the four microphones: physical and virtual microphones on the left and right, $\hat{S}^p{}_{LL}$, $\hat{S}^p{}_{RL}$, $\hat{S}^v{}_{LL}$, $\hat{S}^v{}_{RL}$ are estimated. In stage-2, the right loudspeaker is excited with a similar white noise and accordingly $\hat{S}^p{}_{LR}$, $\hat{S}^p{}_{RR}$, $\hat{S}^v{}_{LR}$ and $\hat{S}^v{}_{RR}$ are estimated. In stage-3, the primary noise is switched on and from the signals at the physical and virtual microphones on the left and right sides, $\hat{H}_L$ and $\hat{H}_R$ are estimated.

COMPARISON OF PREVIOUSLY PROPOSED ALGORITHMS

Three headrest systems are compared in this paper:

1. Conventional ANC headrest system for controlling noise at the physical microphones,

2. Virtual ANC headrest system using the virtual microphone arrangement for controlling noise at the virtual locations,

3. The proposed virtual ANC headrest system using the remote microphone technique based algorithm for controlling noise at the virtual locations.

All three types of headrest system are based on Internal Model Control (IMC) otherwise known as feedback ANC. IMC is a commonly employed control law which uses a model of the plant to estimate the disturbance acting on the plant. In IMC, the reference signal is generated from the error microphone and there is no extra reference microphone present unlike in a feed-forward ANC system. In many practical cases it is impossible to acquire a reference signal as the noise source may be located at a remote location or there may be multiple noise sources. Hence IMC is very beneficial in those circumstances. In addition, IMC simplifies the ANC hardware as it requires fewer microphones and a smaller signal acquisition system.

The conventional ANC headrest system uses the algorithm that is depicted in Fig. 3. This algorithm is designed to minimize the noise at the physically placed error microphones. Conventionally, these error microphones cannot be placed very close to the ear to allow head movement. Cancellation of noise at the physical microphones placed at a distance from the ears does not guarantee noise cancellation at the ear.

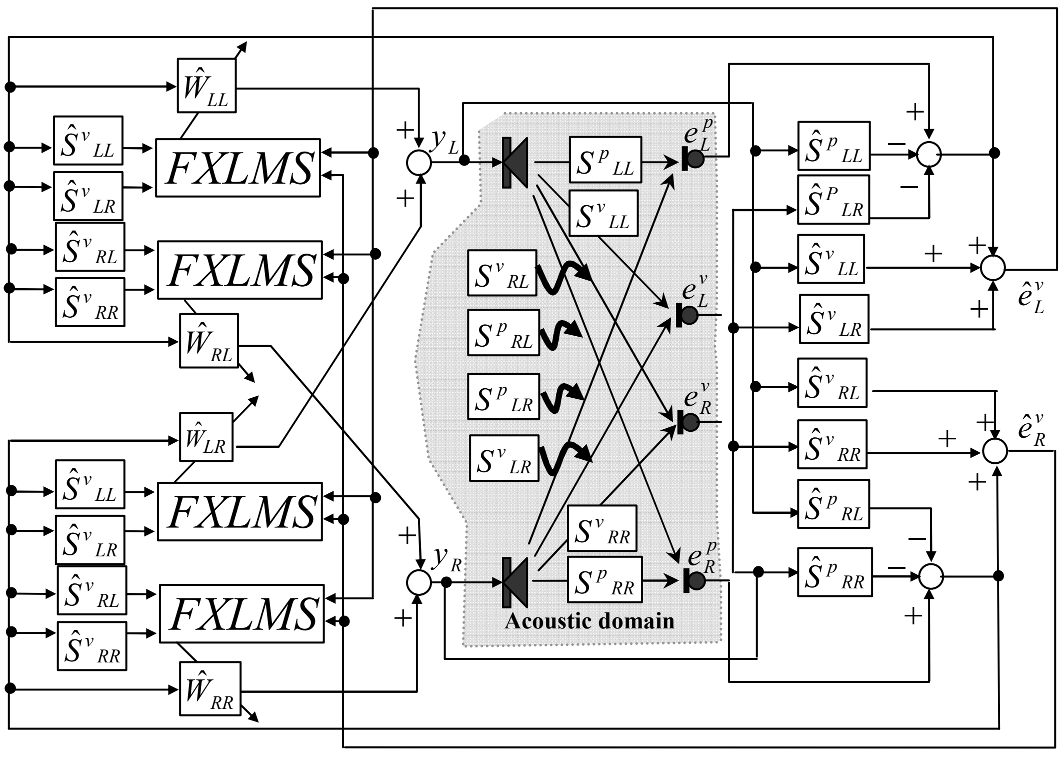

Figure 4 Active headrest algorithm using virtual microphone arrangement.

The virtual ANC algorithm using VMA proposed by Pawelczyk (2003a) is presented in Fig. 4. Comparing Fig. 4 to the proposed algorithm presented in Fig. 2 (b), it can be seen that the proposed algorithm uses an extra transfer function for each side of the headrest to estimate the virtual error signal. This transfer function is the primary transfer function between the physical and virtual microphones on each side. In the algorithm proposed by Pawelczyk (2003a), these transfer functions are unity as it was assumed that the physical and the virtual microphones receive the same noise pressure signal in the case of far-field low-frequency noise, when both the microphones are relatively close. This assumption is not valid in practical cases when the noise source is near to the headrest.

It can be seen from the block diagrams in Fig. 2 to 4 that the computational complexity of the proposed method is a little higher than that of the other two algorithms as two extra transfer functions need to be computed.

EXPERIMENTAL STUDY

The experimental active headrest consists of a manikin whose two ears contain microphones. Two loudspeakers were placed behind the manikin's head. Two physical microphones were placed near the head of the manikin between the speaker and the back of the manikin. This is shown in Fig. 5. The microphones in the ears of the manikin were used as the virtual microphones. A dSpace 1104 ACE kit was used to implement the control algorithm. In this case two DACs were used to drive the two secondary loudspeakers and 4 ADCs were used to collect the microphone signals. A tonal primary noise of frequency 195.65 Hz was generated from a separate system consisting of a signal generator, power amplifier and a loudspeaker. A sampling frequency of 1 kHz was used. The length of all the estimated transfer functions, including the ANC filters was 128. Matlab Simulink codes were written to implement the ANC algorithms. All the three block diagrams presented in Figs. 2 - 4 were implemented. Three orthogonal planes near the ear of the artificial head were scanned by a traverse and the root mean square (RMS) values of the noise amplitude were collected. A 15 × 15 grid of points was collected for each plane which covers an approximate area of 20 × 20 cm. The noise source was placed at a distance of about 470 cm in front of the head. The attenuation in dB was computed as follows

Attenuation (dB) =

$$20\log_{10}[x_{RMS}(ANC)/x_{RMS}(NoANC)], \qquad (7)$$

where $x_{RMS}(ANC)$ is the RMS of the 1000 samples of the scanning microphone signal when the ANC with a particular algorithm is ON and the $x_{RMS}(NoANC)$ corresponds to the same when ANC is OFF.

RESULTS

Figure 6 shows the spatial attenuation in three orthogonal planes near the left side of the head. The figure also shows the relative position of the physical microphone and the head. From Fig. 6 (a) it is apparent that conventional ANC which attenuates the noise at the physical microphone creates a quiet zone towards the upper side of the head as the physical microphone is placed there. With conventional ANC, there is no appreciable attenuation near the ear. With the virtual ANC algorithm based on the VMA technique (Pawelczyk, 2003) the spatial attenuation profile is shown in Fig. 6 (b). This figure shows that this ANC algorithm is incapable of attenuating the noise significantly when in the near-field of the primary source. This attenuation profile is also shown in a reduced scale in Fig. 6 (c). Finally the result obtained using the proposed algorithm is shown in Fig. 6 (d). From Fig. 6 (d) it can be clearly seen that the zone of quiet extends towards the ear as desired. Hence, the proposed RMT based algorithm outperforms the other two algorithms in terms of the attenuation at the ear and the size of the zone of quiet there. The power spectrum magnitude of the microphone signal placed at the left ear of the manikin is plotted in Fig. 7, which shows the comparison of noise reduction capability at the ear of the manikin with all three algorithms. This power spectrum magnitude plot demonstrates about 25 dB reduction in the primary noise (frequency-195.65 Hz) at the ear due to the proposed algorithm which outperforms the other two algorithms.

CONCLUSIONS

This paper has proposed a virtual ANC headrest system using the remote microphone technique. The complete algorithm accompanied by a block diagram has been presented. The algorithm is an internal model control algorithm and hence does not use a reference microphone. The proposed algorithm along with the classical active headrest algorithm and a recently proposed VMA based algorithm has been implemented in real-time. A three dimensional noise attenuation profile was plotted to compare the three algorithms. It is shown that the proposed algorithm outperforms both of these algorithms in terms of noise attenuation near the ear.

ACKNOWLEDGEMENTS

D. P. Das acknowledges the financial support provided by DST, Govt. of India under BOYSCAST Fellowship program to carry out this work at the University of Adelaide. He also acknowledges IMMT, Bhubaneswar and CSIR, India for considering this period of study as deputation and providing full support to him as an employee.

REFERENCES

Brothanek, M, & Jiricek, O 2002, 'Formating of zones of quiet around a head simulator', *Proc. Active-2002*, Southampton, UK, pp. 117-121.

Cazzolato, B 1999, *Sensing systems for active control of sound transmission into cavities*, Ph.D. thesis, School of Mechanical Engineering, The University of Adelaide, SA, 5005, Australia, 1999.

Cazzolato, B 2002, 'An adaptive LMS virtual microphone', *Proc. of Active-2002*, Southampton, UK, 2002, pp. 105-116.

Elliott SJ and David, A 1992, 'A virtual microphone arrangement for local active sound control', *Proc. of the 1st International Conference on Motion and Vibration Control, Yokohama*, pp. 1027-1031.

Garcia-Bonito, J, Elliott, SJ & Boucher, CC 1997, 'Generation of zones of quiet using a virtual microphone arrangement', *J. Acoust. Soc. America*, 101 (6), pp. 3498-3516.

Hansen CH & Synder, SD 1997, *Active control of noise and vibration*, Spon Press, London.

Holmberg, U, Ramnér, N & Slovak, R 2002, 'Low complexity robust control of a headrest system based on virtual microphones and the internal model principle', *Proc. Active-2002*, Southampton, UK, pp. 1243-1250.

Kuo, SM & Morgan, DR 1996, *Active Noise Control Systems, Algorithms and DSP Implementation*, Wiley-Interscience, New York.

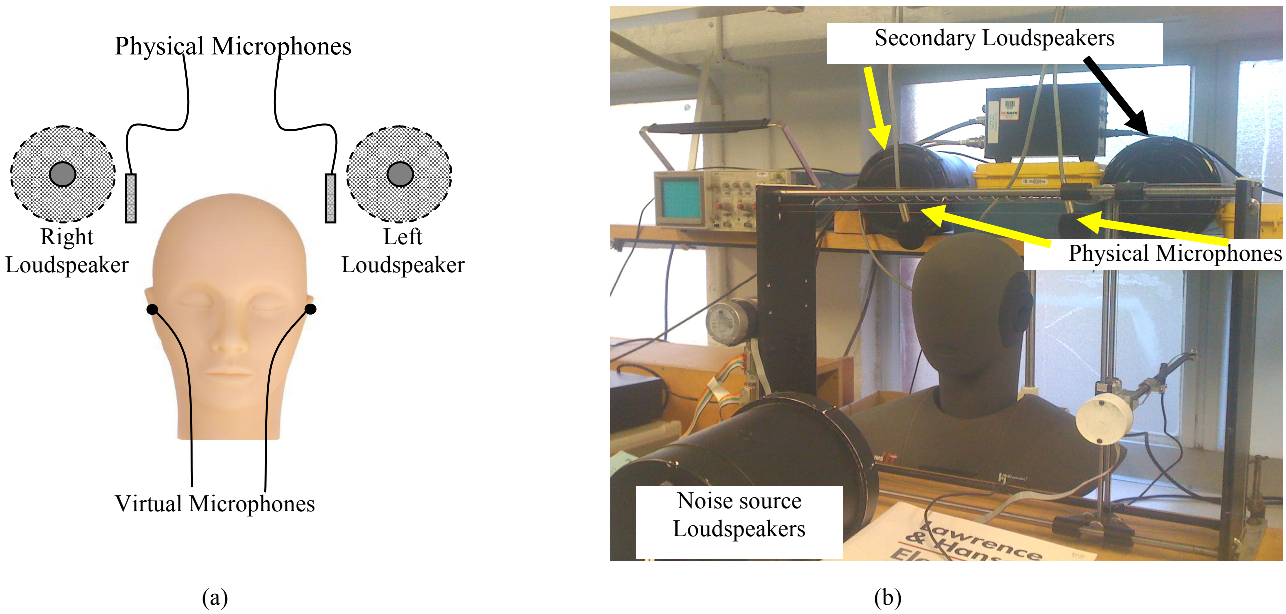

Figure 5 Experimental setup for active headrest (a) schematic diagram (b) photograph.

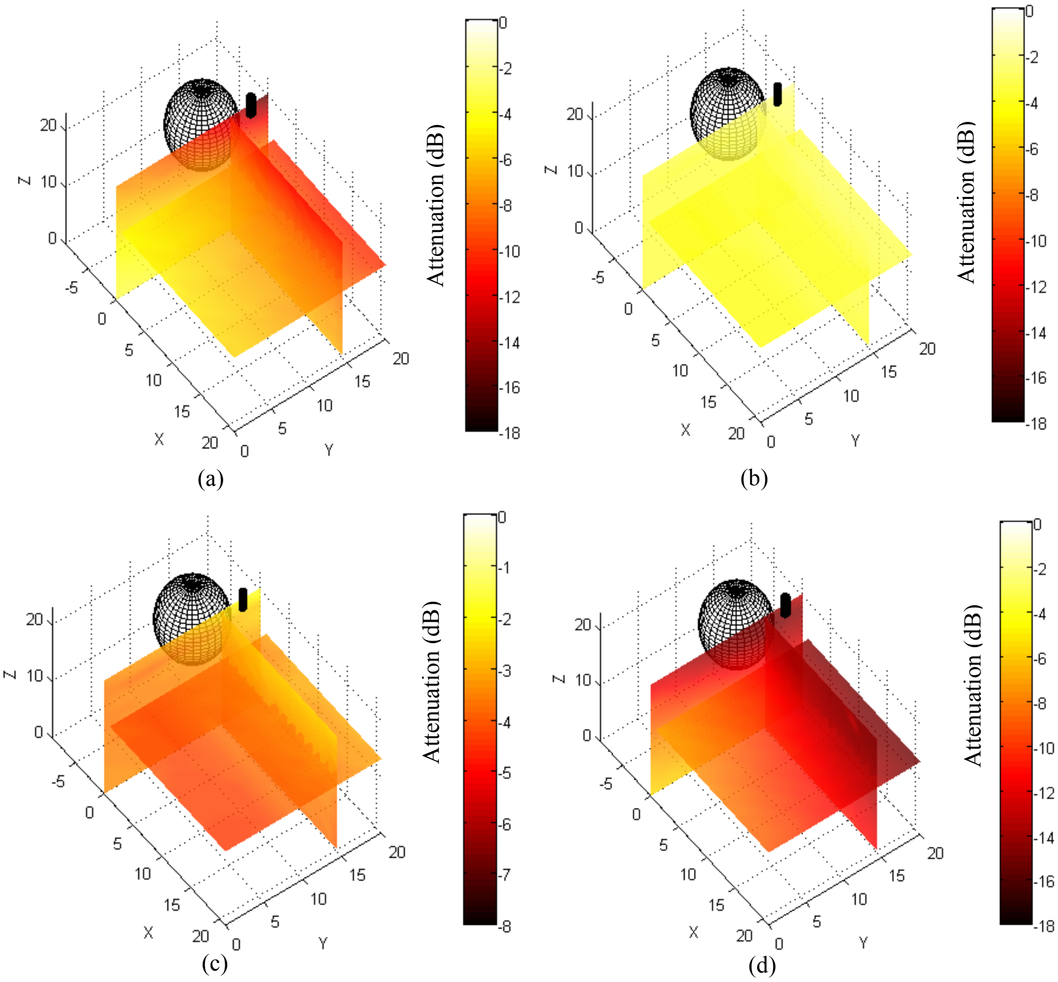

Figure 6 Noise attenuation profile on the left side of the head in three orthogonal planes crossing near the ear (a) Conventional ANC with physical microphone control (b) ANC with VMA Technique (c) ANC with VMA Technique (lower scale) (d) Proposed ANC with RMT. The sphere represents the position of the head, and the cylinder the physical microphone.

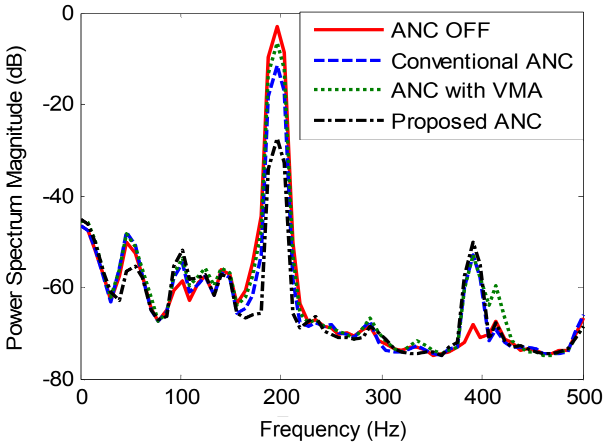

Figure 7 The power spectrum magnitude of the microphone signal placed at the left ear of the manikin.

Moreau, DJ, Ghan, J, Cazzolato, BS & Zander, AC 2009, ‘Active noise control in a pure tone diffuse sound field using virtual sensing’, *Journal of the Acoustical Society of America*, vol. 125, issue 6, pp. 3742-3755.

Nelson, PA & Elliot, SJ 1992, *Active Control of Sound*, Academic Press, San Diego, CA.

Pawelczyk, M 2002a, ‘Control of sound in an active headrest system’, *Proc. IEEE (No. 8119) Conf. MMAR’2002*, Szczecin, Poland, pp. 1157-1162.

Pawelczyk, M 2002b, ‘Control algorithms for locating zones of quiet in the active headrest system’, *Molecular and Quantum Acoustics*, 23, pp. 339-350.

Pawelczyk, M 2003a, ‘Noise control in the active headrest based on estimated residual signals at virtual microphones’, *Proc. Tenth International Congress on Sound and Vibration*, 7-10July 2003, Sweden, pp. 251-258.

Pawelczyk, M 2003b, ‘Multiple input– multiple output adaptive feedback control strategies for the active headrest system: design and real-time implementation’ *Int. J. Adapt. Control Signal Process*. (17) pp. 785–800.

Pawelczyk, M 2004, ‘Adaptive noise control algorithms for active headrest system’, *Control Engineering Practice* (12) pp. 1101–1112.

Petersen, C, Fraanje, R, Cazzolato, B, Zander, A & Hansen, C 2008, ‘A Kalman filter approach to virtual sensing for active noise control’, *Mechanical Systems and Signal Processing*, vol. 22, issue 2, pp. 490-508.

Rafaely, B, Elliott, SJ, & Garcia-Bonito, J 1999, ‘Broadband performance of an active headrests’, *J. Acoust. Soc. America*, 106(2), pp. 787-793.

Rafaely, B & Elliott, SJ, 1999, ‘H2/H-infinity active control of sound in a Headrest: design and implementation’, *IEEE Trans. Control Systems Techn.*, 7(1): pp. 79-84.

Roure, A & Albarrazin, A 2000, ‘The remote microphone technique for active noise control’, *Proc. of Active-1999*, Florida, USA, 2000 pp. 1233–1244.

Tseng, WK, Rafaely, B & Elliott, SJ 2002, ‘Performance limits and real-time implementation of a virtual microphone active headrest’, *Proc. Active-2002*, Southampton, UK, pp. 1231-1242.